Theory of collective spin waves and microwave response of ferromagnetic nanowire arrays

Rodrigo Arias and D. L. Mills
Department of Physics and Astronomy, University of California, Irvine, California 92697
(Received 14 November 2002; published 27 March 2003)

We formulate the theory of the collective spin wave modes and the microwave response of arrays of ferromagnetic nanowires of cylindrical cross section, each magnetized parallel to the axis of symmetry. The theory is based on a multiple scattering approach, and may be applied to the regime where the diameter of the constituents is small enough that exchange enters the response importantly. The formalism can be applied to ordered arrays, or disordered arrays of nanowires. We present explicit results for the spin wave normal mode frequencies of a pair of nanowires, and for a linear array. The dispersion curves for the collective modes in the latter case show a dispersive collective mode which crosses and hybridizes with resonances in the individual cylinders. For a nanowire pair, and in the magnetostatic limit, we obtain a closed form expression for the collective spin wave modes in the limit as the wavevector parallel to the symmetry axis vanishes. Interestingly, the resonance does not split as the wires are brought together, but just shifts downward in frequency, from the value $\gamma(H_0+2\pi M_s)$ appropriate to the isolated wire at large separations, to $\gamma[H_0(H_0+4\pi M_s)]^{1/2}$ when the wires just touch.

DOI: 10.1103/PhysRevB.67.094423 PACS number(s): 75.75.+a, 75.30.Ds, 75.50.−y

I. INTRODUCTION

For well over a decade now, ultrathin films of ferromagnetic material, and multilayers which incorporate such films, have been the topic of intense experimental and theoretical study. The physics in these structures has proved most interesting indeed, and one encounters unique properties not found in bulk magnetic matter. The phenomenon of giant magnetoresistance is perhaps the most commonly discussed such property. But in addition the multilayers offer magnetic response characteristics (hysteresis loops, exotic magnetic structures, microwave response,...) that are both unique, and readily subject to modification through variations in growth conditions, film thickness, and other factors as well. Applications abound, particularly in magnetic recording and data storage, and others are anticipated.

More recently, interest has arisen in other forms of small magnetic structures which, generally speaking, may be described as textured media. For example, two-dimensional arrays of dots exhibit fascinating properties,[1] and the collective excitations of arrays of magnetic stripes show complex and interesting behavior.[2] Our interest in ferromagnetic nanowires has been stimulated by ferromagnetic resonance studies[3] of wires sufficiently small that the resonance spectrum explores modes strongly influenced by exchange, as well as by the Zeeman and magnetic dipole interactions which control the nature of spin waves in larger samples. Our theory[4] of the exchange/dipole modes of such nanowires, along with their microwave response, offers a quantitative explanation of the very interesting doublets observed in the FMR spectra.[3] These have their origin in an exchange induced level crossing between the main FMR mode, and standing spin waves which are driven up in frequency as the wire diameter decreases. The two modes are mixed by boundary conditions at the surface, and as the wire diameter is decreased the frequency of the standing spin wave is driven up through that of the uniform FMR mode. The boundary condition induced hybridization between the two produces the doublet, for diameters near that where crossing occurs. Very recently, a most interesting study[5] of spin waves in a nanowire array by the method of Brillouin light scattering (BLS) provides very clear, quantitative data regarding the dependence of the spin wave frequencies on nanowire diameter, in accord with the expectations in Ref. 4.

Our previous paper was concerned only with properties of an isolated ferromagnetic nanowire. The purpose of this paper is to address the theory of the interactions between ferromagnetic nanowires of cylindrical cross section, when they are incorporated into dense arrays. The issue of interest is the following. First, consider the much studied ferromagnetic film, magnetized parallel to its surface. As the spins precess in the uniform mode normally excited in FMR, they generate a demagnetizing field with origin in ''magnetic charges'' present on the surfaces. These demagnetizing fields are responsible for upshifting the resonance frequency of the film from the precession frequency γH_0 of free spins, to the well known result $\gamma[H_0(H_0+4\pi M_s)]^{1/2}$. Here H_0 is the applied dc magnetic field, and M_s the saturation magnetization of the film. However, the dipole fields so generated are entirely confined to within the film itself. Thus, in a multilayer sample formed of ideal films, the dipolar interactions play no role in coupling adjacent films. If, however, the mode excited has wave vector k parallel to the surface (in BLS experiments, modes with wave vector in the range 10^5 cm^{-1} are excited), then the spin motions generate fields outside the film whose influence scales as $4\pi M_s kd\exp(-kz)$ in the thin film limit, where d is the film thickness, and z the distance from its surface.[6] Such fields are quite weak when $kd \ll 1$, with dipolar interfilm coupling negligible.

However, the uniform mode of a ferromagnetic cylinder generates a field of dipolar character outside its surface, which falls off inversely with the square of the distance from the film center.[4] Under such circumstances, one expects appreciable interactions between nearby nanowires. This suggests that suitable nanowire arrays will offer interesting collective modes, and microwave properties subject to control

by design. It is the purpose of this paper to present the theory of such modes, for nanowires whose diameter is small enough that both exchange and dipolar coupling enter importantly in the response of the individual constituents. We then present numerical studies of selected systems. We provide as well a formulation of the theory of the response of nanowire arrays to spatially uniform applied microwave fields. Motivation for our studies arises from the fact that the experiments in Ref. 3 employed random arrays of ferromagnetic nanowires, so a question regarding the role of interwire interactions on the spectra arises. Also, the most interesting recent experiment cited above[5] which explores the influence of exchange on the spin wave spectra of nanowires, also employed a reasonably dense nanowire structure.

Our basic approach employs multiple scattering theory, in a form adapted to earlier discussions of two-dimensional photonic crystals.[7] Of course, in previous work the application is to dielectric structures which exhibit a scalar dielectric response, whereas here we require an extension to structures composed of ferromagnetic media, whose response is gyrotropic in character. The approach is a real space formulation, and can thus be applied to diverse structures, ranging from those with periodicity similar to photonic crystals, or to disordered structures if desired.

The numerical studies reported here explore two examples. First we discuss a nanowire pair. This serves to quantify the character of the interwire interactions which, in fact to judge by this case, are rather weak. The numerical studies are demanding for the following reason. We consider collective modes characterized by a wave vector *k parallel* to the symmetry axes of the two cylinders. As $k \rightarrow 0$, in our multiple scattering theory, we encounter modified Bessel functions of the form $K_m(kd)$ and $K_m(kR)$, with d and R the distance between the two wires, and their radii, respectively. The function $K_m(x)$ diverges as x^{-m} as $x \rightarrow 0$, so the question of achieving numerical convergence is delicate in the long wavelength limit. We do find we can achieve accurate results for long wavelength modes with modest computing power. Also, we present a scaling argument which allows us to extract equations specific to the limit $k \equiv 0$ from our general formulation. We have a test of our numerical results in the long wavelength limit. Below, we derive an exact, closed form expression for the $k=0$ coupled mode frequencies of the nanowire pair, in the magnetostatic limit. The formula itself is most interesting in character in our view, and also provides us with the means of testing the numerical results at long wavelength by studying wires of substantial diameter, then comparing numerical results to our exact formula. After detailed study of the nanowire pair we turn our attention to a linear array of nanowires. These calculations are motivated by the BLS studies of linear arrays of magnetic stripes.[2] While our nanowire arrays are very different than the stripes studied by Demokritov *et al.*,[2] we are motivated by issues raised in these studies. Most strikingly, in the data a mode very similar in character to the well known Damon Eshbach mode of the thin ferromagnetic film is observed. This mode crosses and hybridizes with the standing wave exchange modes of the individual constituents of the array. We find results strikingly similar to these in our study of the one-dimensional line of cylinders. It is the case, incidentally, that linear ferromagnetic nanowire arrays can be grown on crystal surfaces. When magnetic ions are deposited on stepped surfaces, they may migrate to step edges thus forming a linear array of ferromagnetic nanowires with nanoscale diameter.[8]

The outline of this paper is as follows. Section II is divided into two parts. We first, through use of multiple scattering theory, develop an approach to the description of the spin wave excitations of an array of parallel nanowires, each assumed of cylindrical cross section, and magnetized parallel to its symmetry axis. In the second part, we develop a description of the response of such an array to an external driving field. Both of these treatments fully incorporate (within long wavelength phenomenology) the influence of exchange, and of surface anisotropy fields on the response of the individual constituents in the array. It should be remarked that in this section, we borrow from results and concepts introduced in our earlier paper[4] on the spin excitations and microwave response of the isolated nanowire. Our numerical results are presented in Sec. III, and concluding comments are in Sec. IV. In an Appendix we present the analytic derivation of the resonance frequency of two nanowires whose centers are separated by the distance d, for the case where their diameters are large enough for magnetostatic theory to apply.

II. THEORY OF THE SPIN EXCITATIONS AND THE MICROWAVE RESPONSE OF FERROMAGNETIC NANOWIRE ARRAYS

We consider an array of nanowires of cylindrical cross section, each with radius R, each with symmetry axis parallel to the z axis, and each magnetized along the symmetry axis with magnetization per unit volume M_s. Our formulation of the response of the array is a real space formulation, and thus it is not necessary to assume the wires form a two-dimensionally periodic array or any other special structure. While we suppose here all wires in the array are identical in radii and properties, in fact it is straightforward to incorporate variations in radii and magnetization from wire to wire into the analysis if desired. The extension to the case where the applied dc magnetic field has a transverse component is nontrivial, however.

If we consider the motion of the magnetization in one particular wire, then as discussed in our earlier paper,[4] a dynamic magnetic dipole field is generated in the spatial region outside the wire by the precession of the magnetization. If the nanowires are separated by distances greater than the atomic length scale, then the interaction between the wires will be controlled by this dynamic dipole field, as opposed to interwire exchange interactions of microscopic origin. Our treatment includes, in the description of the response of the array, the influence of intra-wire exchange, and also the role of surface anisotropy fields on the response of a single entity in the array. We confine our attention to the limit where the separation between adjacent wires is sufficiently large that interactions between them occur only via the dipolar mechanism.

A. Theory of the collective spin wave excitations of an array of cylindrical nanowires

Suppose we have an array of nanowires such as described in the previous two paragraphs. Translational symmetry in the z direction insures that the collective excitations of the array are characterized by a wave vector parallel to the $\hat{z}$ axis we may call k. Thus, the dipolar field generated by the precession of the magnetization vectors in the various wires may be written everywhere as $\vec{h}_d(\vec{r},t)=\vec{h}_d(x,y)\exp[ikz-i\Omega_\alpha(k)t]$, where $\Omega_\alpha(k)$ is the frequency of the mode of wave vector k. The subscript α is a branch index, since for each choice of k one finds a hierarchy of branches. It will suffice, for the small arrays of interest here to calculate the dipole field in the magnetostatic approximation, where retardation effects are ignored. Thus, we will have $\vec{h}_d(\vec{r},t)=-\nabla\varphi_M(\vec{r},t)$ where $\varphi_M(\vec{r},t)=\Phi_M(x,y)\exp[ikz-i\Omega_\alpha(k)t]$ is the magnetic scalar potential.

Now in the vacuum region between nanowires, the magnetic potential obeys Laplace's equation, so for the function $\Phi_M(x,y)$ everywhere outside the nanowires we have

$$\left(\frac{\partial^2}{\partial x^2}+\frac{\partial^2}{\partial y^2}\right)\Phi_M(x,y)-k^2\Phi_M(x,y)=0. \tag{1}$$

Before we turn to the nanowire array, let us consider a simpler problem, the response of a single nanowire centered at the origin of the coordinate system in the xy plane to an externally applied driving field, itself described by the magnetostatic approximation just discussed. We may express the function $\Phi_M^{(ext)}$ from which the external field is described in terms of polar coordinates (ρ,ϕ) in the xy plane. We may express $\Phi_M^{(ext)}(\rho,\phi)$ as an expansion in modified Bessel functions:

$$\Phi_M^{(ext)}(\rho,\phi)=\sum_{n=-\infty}^{\infty}A_n(0)I_n(k\rho)\exp(in\phi). \tag{2}$$

Since the external potential is generated by sources outside the near vicinity of the origin of the coordinate system, the potential must be nonsingular there.

The external potential in Eq. (2) will excite the magnetization of the nanowire at the origin. The resulting precession will generate a dynamic dipole field outside this object. This external field may be calculated through use of a very straightforward extension of the formalism described in Sec. II A of Ref. 4. We do not present the details here in the interest of brevity. The field outside the wire may be generated from the potential

$$\Phi_M^{(0)}(\rho,\phi)=\sum_{n=0}^{\infty}A_n(0)S_nK_n(k\rho)\exp(in\phi) \tag{3a}$$

or

$$\Phi_M^{(0)}(\rho,\phi)=\sum_{n=-\infty}^{\infty}B_n(0)K_n(k\rho)\exp(in\phi). \tag{3b}$$

We have $B_n(0)=S_nA_n(0)$, where S_n, equivalent to the S matrix of scattering theory, describes the response of the nanowire to a driving field with azimuthal variation $\exp(in\phi)$. In Eqs. (3), $K_n(x)$ is the modified Bessel function of the second kind. Since, for large x, we have $K_n(x)\sim\exp(-x)/x^{1/2}$, the field generated by the motion of the magnetization falls off exponentially as we move away from the nanowire, with range controlled by the magnitude of the wave vector. As the wave vector k vanishes, the behavior of the scalar potential is controlled by the small argument form of $K_n(x)$. Since for nonzero values of n, $K_n(x)$ is proportional to x^{-n} we have a power law fall off of the field. In FMR studies of the isolated cylinder, the $m=1$ mode is excited,[4] so for this case the magnetic potential falls off inversely with the distance from the center of the cylinder, and the dipole field itself falls off inversely with the square of this distance.

In Ref. 4, one finds the formalism for constructing S_n within a framework that includes exchange effects inside the nanowire, and which includes the role of surface anisotropy as well. The latter is incorporated into the boundary conditions satisfied by the transverse magnetization. We find that

$$S_n=-\frac{[G_nI_n(kR)-k\Gamma_nI_n(kR)']}{[G_nK_n(kR)-k\Gamma_nK_n(kR)']}, \tag{4a}$$

where in the magnetostatic limit one has

$$G_n^{(mag)}=\left[\left(\frac{n\mu_2}{R}\right)I_n(\tilde{k}R)-\mu_1^{1/2}kK_n(\tilde{k}R)'\right] \tag{4b}$$

and

$$\Gamma_n^{(mag)}=-I_n(\tilde{k}R). \tag{4c}$$

For the case exchange and surface anisotropy are both present, we have

$$G_n^{(ex)}=\sum_{j=1}^{3}\kappa_jA_j^n\left[2\pi M_s\left\{\frac{J_{n+1}(\kappa_jR)}{D(\kappa_j^2+k^2)+H_0+\Omega}-\frac{J_{n-1}(\kappa_jR)}{D(\kappa_j^2+k^2)+H_0-\Omega}\right\}-J_n(\kappa_jR)'\right] \tag{4d}$$

and

$$\Gamma_n^{(ex)}=-\sum_{n}^{3}A_j^nJ_n(\kappa_jR). \tag{4e}$$

In Eqs. (4a)–(4c), $I_n(x)$ is the modified Bessel function of the first kind, and the prime on the various Bessel functions denotes derivatives with respect to their argument. The quantity $\mu_1=(\Omega_B\Omega_H-\Omega^2)/(\Omega_H^2-\Omega^2)$ while $\mu_2=-4\pi\Omega_M\Omega/(\Omega_H^2-\Omega^2)$, where $\Omega_H=\gamma H_0$, $\Omega_M=\gamma M_s$, and $\Omega_B=\gamma(H_0+4\pi M_s)$, with γ the gyromagnetic ratio (its modulus), and H_0 the strength of the dc magnetic field applied parallel to the cylinder axis. Finally, $\tilde{k}=k/\mu_1^{1/2}$. In Eqs. (4d) and (4e), the κ_j are the roots of Eq. (16) of Ref. 4, and D is the exchange stiffness. The coefficients A_j^n, analogous

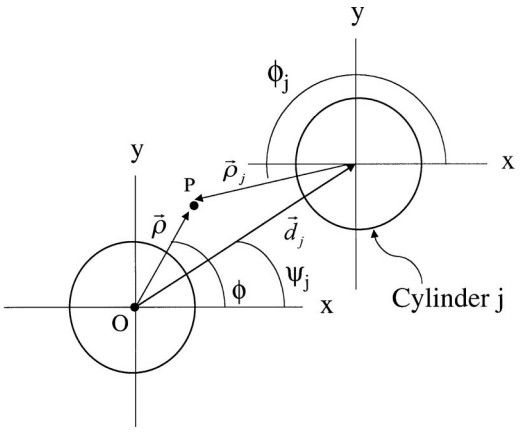

FIG. 1. An illustration of the coordinate system and variables employed in the formal development in Sec. II.

to the coefficients A_i in Eq. (17) of Ref. 4 are determined as follows. First set A_1^n to unity, and determine the two remaining coefficients by requiring the two boundary conditions in Eq. (21a) and Eq. (21b) of Ref. 4 to be satisfied. With A_1^n set to unity, these can be arranged to be two inhomogeneous equations for the two remaining coefficients.

Now consider an array of nanowires, with the origin of the coordinate system placed at the center of one selected wire. If a collective excitation is excited in the array, the magnetization of the wire at the origin is driven by the dynamic dipolar fields generated by the other wires in the array. We shall obtain a self-consistent set of equations for the amplitude of the motion in any particular wire by casting the driving field from the remainder of the array in a suitable form. This is our next task.

In Fig. 1, we show the cylinder at the origin, and one of the cylinders in the array, cylinder j. The magnetization of the cylinder at the origin is driven by the field calculated from the magnetic potential

$$\tilde{\Phi}_M(x,y)=\sum_{j\neq 0}\sum_{n=-\infty}^{+\infty} B_n(j)K_n(k\rho_j)\exp(in\phi_j). \tag{5}$$

We will manipulate Eq. (5) to cast it in a form which allows contact with our discussion of the isolated cylinder driven by an external field. One begins with Graf's identity, which reads[9]

$$e^{iv\psi}Z_v(kR)=\sum_{n=-\infty}^{\infty} Z_{v+n}(kr)J_n(k\rho)e^{in\varphi}. \tag{6}$$

In Eq. (6), $\vec{\rho}$ and $\vec{r}$ are vectors, with $\rho=|\vec{\rho}|<r=|\vec{r}|$, φ is the angle between these two vectors, ψ is the angle opposite to $\vec{\rho}$, in a triangle formed by $\vec{\rho}$, $\vec{r}$ and a line drawn between the tips of these two vectors, while $R=(r^2+\rho^2-2r\rho\cos(\varphi))^{1/2}$. The function $Z_v(x)$ can be any of the standard Bessel functions (Bessel, Neuman, and Hankel). Upon choosing Z_v to be the Hankel function of the first kind, $H_v^{(1)}$, and then letting $k\rightarrow ik$, one finds that

$$e^{iv\psi}K_v(kR)=\sum_{n=-\infty}^{+\infty} K_{v+n}(kr)I_n(k\rho)e^{in\varphi}. \tag{7}$$

Upon consulting Fig. 1, and identifying R with ρ_j of that figure, we have the relation

$$e^{iv\phi_j}K_v(k\rho_j)=(-1)^v\sum_{n=-\infty}^{+\infty} e^{i(v-n)\psi_j}K_{v-n}(kd_j)I_n(k\rho)e^{in\phi}. \tag{8}$$

The quantities which appear in Eq. (8) are all defined in Fig. 1. To obtain Eq. (8) from Eq. (7), note that $K_{-v}(x)=K_v(x)$. When Eq. (8) is combined with Eq. (5), we have

$$\tilde{\Phi}_M(x,y)=\sum_{n=-\infty}^{+\infty}\tilde{A}_n(0)I_n(k\rho)e^{in\phi}, \tag{9}$$

where

$$\tilde{A}_n(0)=\sum_{j\neq 0}\sum_{m=-\infty}^{\infty}(-1)^m e^{i(m-n)\psi_j}B_m(j)K_{m-n}(kd_j). \tag{10}$$

Now the driving potential displayed in Eq. (9) excites the magnetization in the cylinder at the origin, and it produces a disturbance outside the cylinder at the origin described by the magnetic potential given in Eq. (3b), with

$$B_n(0)=S_n\tilde{A}_n(0), \tag{11}$$

so we have a set of equations that link the amplitudes $B_n(j)$:

$$S_n^{-1}B_n(0)=\sum_{j\neq 0}\sum_{m=-\infty}^{\infty}(-1)^m e^{i(m-n)\psi_j}K_{m-n}(kd_j)B_m(j). \tag{12}$$

The statement in Eq. (12) is the principal result of the present section. For the isolated cylinder, the frequencies of the spin wave eigenmodes associated with the azimuthal quantum number n are found by locating the poles of S_n, or equivalently the zeros of S_n^{-1}. In the limit the cylinders are infinitely far apart, Eq. (12) provides this criterion. For an array of cylinders, the modes cannot be characterized by this azimuthal quantum number, and become mixed in character. One finds the frequencies of the various modes of the array with the wave vector k by locating the zeros of the determinant formed from Eq. (12). In practice, one takes a finite range of n in the sum, ranging from $-N$ to $+N$ so the size of the determinant whose zeros must explore is $2N+1$ multiplied by the number of cylinders in the sample. Of course, if one has a periodic array, the coefficients $B_n(j)$ will have a Bloch form, i.e., $B_n(j)=B_n(0)\exp(i\vec{k}_\perp\cdot\vec{d}_j)$, so for each wave vector $\vec{k}_\perp$ one explores a determinant whose size is $2N+1$.

For many purposes, it is of interest to explore the spin wave excitations for which the wave vector k is zero. If we consider a true nanoscale sized array of wires excited in FMR or in BLS, the modes of interest will have wavelengths very long compared to the length scales of the structure, and thus the limit of vanishing k is of primary interest. The matrix formed from Eq. (12) whose determinant is evaluated

numerically is very tricky to evaluate at very small values of the wave vector, since as noted before $K_n(x)$ diverges as x^{-n} as $x \to 0$. If one truncates the matrix with a large value of N, then the matrix will contain modified Bessel functions of very large order. For small values of the wave vector, there will be very large entries in the matrix, and by and large these are associated with partial waves that play a minor role in the final result, if N is large enough to insure excellent convergence. Despite this concern, in the calculations reported in Sec. III, in our studies of the normal modes of two cylinders we have had no difficulty achieving accurate results for with $N=30$, and kR as small as 10^{-3}. It is surprising to us that high accuracy can be obtained at such very small values of kR, in view of the behavior of the modified Bessel functions in the limit of small argument.

In case where the response of the individual wires is adequately described by magnetostatic theory, with the influence of exchange ignored [thus S_n is given by Eq. (4)], as $k \to 0$, through appropriate scaling arguments it is possible to extract the limiting behavior of the various quantities that enter Eq. (12), and reduce it to a form which may be used to compute the $k=0$ mode frequencies directly. Since these equations allow direct calculation of the mode frequencies without the issue just discussed, we conclude with a derivation of the resulting equation. We assume that S_n is given by Eq. (4) and that we have $kR \ll 1$ and $kd_j \ll 1$ as well. Recalling that when $kd_j \ll 1$, we have, for $n>0$,

$$K_{-n}(kd_j) = K_n(kd_j) \approx \frac{2^{n-1}(n-1)!}{(kd_j)^n}, \tag{13}$$

while in the same limit, $K_0(kd_j) \approx \ln(2/kd_j)$. After some algebra, one may show that when $kR \ll 1$, one has, for $n \neq 0$,

$$S_n \approx \frac{2|n|(kR)^{2|n|}}{4^{|n|}(n!)^2} \frac{[1+\mu_2 \mathrm{sgn}(n)-\mu_1]}{[1-\mu_2 \mathrm{sgn}(n)+\mu_1]} = s_n k^{2|n|}, \tag{14}$$

while again in the same limit, $S_0 \approx \frac{1}{32}[(1/\mu_1)-1](kR)^4 = s_0 k^4$.

These forms suggest that the coefficients $B_n(j)$ should exhibit a power law scaling with the wave vector, in the long wavelength limit. We make the ansatz

$$B_n(j) = k^{|n|} b_n(j). \tag{15}$$

When these various limiting forms are inserted into Eq. (12), the result may be arranged to read, for $n \neq 0$,

$$b_n(0) = s_n k^{|n|} \sum_{j \neq 0} \left\{ (-1)^n k^{|n|} \ln\left(\frac{2}{kd_j}\right) b_n(j) + \sum_{m=n+1}^{\infty} (-1)^m \frac{\Lambda_{m-n}}{k^{|m-n|}} k^{|m|} b_m(j) + \sum_{m=-\infty}^{n-1} (-1)^m \frac{\Lambda_{m-n}}{k^{|m-n|}} k^{|m|} b_m(j) \right\}, \tag{16a}$$

where

$$\Lambda_{m-n} = \frac{2^{(|m-n|-1)}(|m-n|-1)!}{(d_j)^{|m-n|}} e^{i(m-n)\psi_j}. \tag{16b}$$

If one writes out the equation satisfied by $b_0(0)$ then takes the limit $k \to 0$, then one finds $b_0(0)=0$. Since there is nothing special about the nanowire located at the origin of the coordinate system, it follows that for all j, $b_0(j)=0$.

To proceed further, one must separate two cases, $n>0$ and $n<0$. When this is done, and the limit of vanishing wave vector is taken, then we obtain two sets of coupled equations in which the wave vector is absent:

$$b_{|n|}(0) = s_{|n|} \sum_{j \neq 0} \sum_{m=1}^{\infty} (-1)^m e^{-i(m+|n|)\psi_j} \times \frac{2^{|n|+m-1}(|n|+m-1)!}{(d_j)^{|n|+m}} b_{-|m|}(j) \tag{17a}$$

and

$$b_{-|n|}(0) = s_{-|n|} \sum_{j \neq 0} \sum_{m=1}^{\infty} (-1)^m e^{i(|n|+m)\psi_j} \times \frac{2^{|n|+m-1}(|n|+m-1)!}{(d_j)^{|n|+m}} b_{|n|}(j). \tag{17b}$$

Once again, if the nanowires are arranged in the form of a periodic structure, one may seek solutions of Eqs. (17) of the Bloch form. There is considerable interest in propagation perpendicular to the magnetization in arrays such as considered here, since in this geometry, nonreciprocal propagations characteristics are exhibited by the system. In two-dimensionally periodic arrays, Eqs. (17) may be used to explore such issues. We have found the limiting forms in Eqs. (17) most useful in the calculations reported in Sec. III.

The derivation of Eqs. (17a) is valid only when intrawire exchange is ignored, and the response of the individual wires is described adequately by magnetostatics as discussed earlier. One may apply the scaling argument to the case where intra wire exchange is included as well. One notes that of the roots κ_j, one of these which we may denote by κ_1 will vanish linearly with k in the limit $k \to 0$ while the other two roots remain finite. We do not present the details of the derivation here. We have found Eqs. (17) most useful in our numerical work, whereas the scaled equations with intrawire exchange were not so easy to explore. We obtained excellent long wavelength results, as reported below, with the full set of equations and the wave vector k set to a small value in the calculations which include intrawire exchange.

B. Response of nanowire arrays to microwave excitation fields

In this section, we present the theory of the response of an array of nanowires to a microwave exciting field, for the case where the magnetic field associated with the incident microwaves lies in the xy plane, perpendicular to the axis of sym-

metry of the wires in the array. As above, we assume all elements in the array are magnetized parallel to their axes of symmetry.

As in Ref. 4, it is particularly convenient to describe the fields in the externally generated microwaves through use of a vector potential $\vec{A}(x,y;t)=\hat{z}A(x,y)\exp(-i\Omega t)$. The magnetic field then lies in the plane, and in addition we have an electric field associated with the incident field parallel to the axis of symmetry. The choice

$$A^{(ext)}(x,y)=\frac{h_0}{ik_0}\exp(i\vec{k}_0\cdot\vec{r}), \tag{18a}$$

with $\vec{k}_0=k_0(\cos\theta_0\hat{x}+\sin\theta_0\hat{y})$ and $k_0=\Omega/c$, describes a microwave field with strength h_0. The magnetic field in the wave is given by

$$\begin{aligned}\vec{B}^{(ext)}=\vec{H}^{(ext)}&=\vec{\nabla}\times\vec{A}\\&=h_0[\hat{x}\sin(\theta_0)-\hat{y}\cos(\theta_0)]\exp(i\vec{k}_0\cdot\vec{r}-i\Omega t),\end{aligned} \tag{18b}$$

with, as noted above, an electric field $\vec{E}^{(ext)}=ik_0\vec{A}$ parallel to the $\hat{z}$ axis. Note that the function $A(x,y)$ in Eq. (18) may be written in the form, with ρ and ϕ polar coordinates in the plane:

$$\begin{aligned}A^{(ext)}(x,y)&=\frac{h_0}{ik_0}\exp[ik_0\rho\cos(\phi-\theta_0)]\\&=\frac{h_0}{ik_0}\sum_{n=-\infty}^{\infty}(i)^nJ_n(k_0\rho)\exp[in(\phi-\theta_0)].\end{aligned} \tag{19}$$

This section presents the theory of the response of the nanowire array to the microwave exciting field just described. In Ref. 4, the theory of the response of a single nanowire to such a field was presented, and here, using logic similar to that in the previous section, we expand the discussion to an array of interacting nanowires. Primary interest resides in the case where the wavelength of the exciting field is very long compared to the length scales of the sample, so after generating the general theory, using scaling arguments similar to those presented above, we also derive equations appropriate to the limit $k_0\to 0$, with the frequency Ω kept finite (formally, one achieves this limit by allowing the velocity of light c to become infinite). To achieve this limit, some rather subtle issues are encountered. Thus, we will want to generalize the expression in Eq. (19) to read

$$A^{ext}(\rho,\phi)=\frac{h_0}{ik_0}\sum_{n=-\infty}^{\infty}(i)^n\lambda_nJ_n(k_0\rho)\exp[in(\phi-\theta_0)]. \tag{20}$$

We recover response to a plane wave by setting all parameters λ_n to unity, but as we take the limit $k_0\to 0$ another choice will be dictated by physical considerations described below.

We again focus our attention on the cylinder located at the origin of the coordinate system, as depicted in Fig. 1. The magnetization of this cylinder is driven by the external field just described, but we must add to this the magnetic fields generated by the precession of the magnetization within other cylinders of the array. The field generated by the precession of the magnetization in a given cylinder has, in the language of scattering theory, the character of an outgoing wave. It is the case that the magnetic fields associated with these waves all lie in the xy plane, and the associated vector potential is thus parallel to the z direction, and is given by $\vec{A}=\hat{z}\tilde{A}$, where

$$\tilde{A}=\sum_{j=0}\sum_{m=-\infty}^{\infty}b_m(j)(i)^me^{im\phi_j}H_m^1(k_0\rho_j), \tag{21}$$

where $H_m^1(x)$ is the Hankel function of the first kind. Through appropriate use of Graf's identity once again [Eq. (6) above], we may cast this in a form which describes a driving field similar in structure to that in Eq. (20). The total vector potential which drives the magnetization of the cylinder located at the origin can then be cast in the form

$$\begin{aligned}A^{(tot)}(\rho,\phi)=\sum_{n=-\infty}^{\infty}\Bigg[&\frac{h_0}{ik_0}\lambda_ne^{-in\theta_0}+\sum_{j\neq 0}\sum_{m=-\infty}^{\infty}b_m(j)\\&\times(i)^{m-n}e^{+i(m-n)\psi_j}H_{n-m}^1(k_0d_j)\Bigg]\\&\times(i)^nJ_n(k_0\rho)e^{in\phi}.\end{aligned} \tag{22}$$

If the cylinder at the origin is subjected to a driving field generated from a vector potential of the form

$$A^{(in)}=\sum_{n=-\infty}^{\infty}a_n(0)(i)^nJ_n(k_0\rho)e^{in\phi}, \tag{23}$$

the precession of its magnetization produces the outgoing field

$$A^{(out)}=\sum_{n=-\infty}^{\infty}b_n(0)(i)^nH_n^1(k_0\rho)e^{in\phi}, \tag{24}$$

where $b_n(0)=Z_na_n(0)$, where the response function Z_n is that of a single nanowire. A prescription for constructing Z_n is found in Ref. 4, within the framework of a description that included the influence of both exchange, and uniaxial surface anisotropy on the response characteristics of the nanowire. We shall discuss the structure of this response function below, since we will need to understand its behavior as we let $k_0\to 0$.

By combining Eq. (22) with the definition of Z_n, we obtain a set of equations from which the amplitudes $b_n(j)$ of the various cylinders may be determined:

$$\begin{aligned}b_n(0)=Z_n\Bigg[&\frac{h_0}{ik_0}\lambda_ne^{-in\theta_0}+\sum_{j\neq 0}\sum_{m=-\infty}^{\infty}b_m(j)\\&\times(i)^{m-n}e^{i(m-n)\psi_j}H_{n-m}^1(k_0d_j)\Bigg].\end{aligned} \tag{25}$$

If there are N nanowires in the array, then we may generate N inhomogeneous equations of the type given in Eq. (25) for the amplitude of the response of each nanowire. Inversion of the matrix formed from this set of equations provides us with a description of the microwave response of the system. The size of this matrix is $N(2M+1)$, where M is the cutoff chosen for the index m in $b_m(j)$.

However, as noted above, there will be considerable interest in the long wavelength limiting form of the response, if the wavelength of the exciting field is very long compared to the physical length scales in the system. While Eqs. (25) are surely exact, it can be a numerical challenge to perform the inversion, since in the limit of small arguments, $H_m^1(x)$ diverges as x^{-m}. Thus, as in our discussion of the collective excitations of the system, it is very useful to have in hand a set of equations applicable to the limit $k_0 \equiv 0$.

For this purpose, we need to understand the structure of the response function Z_n in the limit $k_0 R \ll 1$. We should comment again on the nature of the limit we shall take. Of interest is the case where the wavelength of the exciting radiation is very long compared to all length scales in the structure. However, it is important for the frequency Ω to remain finite and arbitrary, since clearly we are interested in the resonant response of the structure. Thus, upon noting that $k_0 = \Omega/c$, we have in mind the limit $c \to \infty$ with Ω fixed. In the previous section on collective excitations, we made statements about the structure of S_n in this limit but only in the magnetostatic limit, i.e., we did not include the influence of exchange on the response of the isolated nanowire in the discussion presented there. In the present instance, we can derive the long wavelength limiting form of the equations in the general case, and they prove most useful. First, as discussed in Sec. II B of Ref. 4, the various fields, along with the magnetization components inside a given nanowire can be determined from the vector potential within the wire. We write this in the form, with the nanowire at the origin of the coordinate system in mind, $\vec{A}^<(\rho,\phi) = \hat{z}A^<(\rho,\phi)\exp(-i\Omega t)$ where here we write the most general structure for $A^<$ in the form, selecting out just the piece with angular variation characterized by the azimuthal quantum number n,

$$A_n^<(\rho,\phi) = a_n^< \left\{ \sum_{i=1}^{3} \Lambda_n^i J_n(\kappa_i \rho) e^{in\phi} \right\}. \tag{26}$$

The wave vectors κ_i, which are functions of the frequency Ω (and not $k_0 = \Omega/c$) are found by solving Eq. (31) of Ref. 4. The coefficients Λ_n^i are found as follows. First, set Λ_n^1 to unity. Then the remaining two coefficients may be determined from the two boundary conditions on the transverse magnetization stated Eqs. (21) of Ref. 4. These are both homogeneous boundary conditions, but become two inhomogeneous equations in two unknowns, if one sets Λ_n^1 to unity. After this is done, Eq. (26) contains the one free parameter $a_n^>$. The electromagnetic boundary conditions remain. The continuity of the vector potential at $\rho = R$ insures the continuity of the tangential electric field (the z component) at the surface, and the radial component of the magnetic induction $B_\rho = (1/\rho)(\partial A/\partial \phi)$. We then have continuity of the tangential component of $\vec{H}$, H_ϕ. The azimuthal component of $\vec{H}$ inside the wire is generated by calculating B_ϕ from the vector potential, then using Eq. (33b) of Ref. 4 to obtain m_ϕ, the azimuthal component of magnetization. The solutions inside are then matched to the linear combination

$$A_n^>(\rho,\phi) = [a_n J_n(k_0\rho) + b_n H_n^1(k_0\rho)] e^{in\phi} \tag{27}$$

outside the wire. Then the response function Z_n is found from the ratio b_n/a_n.

This procedure yields the following form:

$$Z_n = -\frac{[G_n J_n(k_0 R) - \Gamma_n k_0 J_n(k_0 R)']}{[G_n H_n^1(k_0 R) - \Gamma_n k_0 H_n^1(k_0 R)']}. \tag{28}$$

In Eq. (28), the quantities G_n and Γ_n are functions of frequency Ω, but are independent of k_0. Thus, all the dependence of Z_n on k_0 is displayed explicitly in Eq. (28). Explicit expressions for G_n and Γ_n are as follows:

$$\Gamma_n = \sum_{i=1}^{3} \Lambda_n^i J_n(\kappa_i R) \tag{29a}$$

and

$$G_n = \sum_{i=1}^{3} \kappa_i \Lambda_n^i \left\{ J_n(\kappa_i R)' + 2\pi M_s \times \left[\frac{J_{n+1}(\kappa_i R)}{\tilde{B}_0 + D\kappa_i^2 + \Omega} - \frac{J_{n-1}(\kappa_i R)}{\tilde{B}_0 + D\kappa_i^2 - \Omega} \right] \right\}. \tag{29b}$$

In Eq. (29b), D is the spin wave exchange stiffness, and $\tilde{B}_0$ is defined in Ref. 4.

It's now a straightforward matter to take the limit $k_0 \to 0$ in the expression for Z_n. We must distinguish between $n \neq 0$ and $n = 0$. For the case where $n \neq 0$, in the limit that $k_0 \to 0$ we find

$$Z_n = \frac{\pi}{i} \frac{|n|(k_0 R)^{2|n|}}{4^{|n|}(|n|!)^2} z_n, \tag{30a}$$

with

$$z_n = \left(\frac{RG_n - |n|\Gamma_n}{RG_n + |n|\Gamma_n} \right), \tag{30b}$$

where in the same limit we have

$$Z_0 = -\frac{i\pi}{2} \frac{1}{\ln(1/k_0 R)}. \tag{30c}$$

Now we encounter a tricky issue. If we set all λ_n to unity in Eq. (20) then take the limit $k_0 \to 0$, the externally applied vector potential reduces to the form $\hat{z}(h_0/ik_0)\exp(i\Omega t)$. This describes a spatially uniform *electric* field parallel to the z axis, and in fact the magnetic field vanishes. We thus have a physically incorrect limit. We address this by setting $\lambda_0 = 0$ everywhere, and all other λ_n to unity. Then as $k_0 \to 0$ the

vector potential, parallel to $\hat{z}$ of course, has amplitude given by the expression $h_0\rho\cos(\phi-\theta_0)\exp(-i\Omega t)$. This describes an externally applied magnetic field in the xy plane as desired, given by $h_0(\hat{x}\sin\theta_0-\hat{y}\cos\theta_0)\exp(-i\Omega t)$, and the strength of the electric field vanishes in the limit $k_0\to 0$. In the limit, the coefficients $b_m(j)$ in Eq. (25) exhibit the scaling behavior

$$b_m(j)=(k_0R)^{|m|}\beta_m(j). \tag{31}$$

When we take the limit $k_0\to 0$, the equation satisfied by $\beta_0(0)$ reduces to

$$\beta_0(0)+\sum_{j\neq 0}\beta_0(j)=0, \tag{32}$$

so we may choose $\beta_0(j)=0$ for all j. We then find, in the limit $k_0\to 0$, for $n>0$

$$\beta_n(0)=-\frac{\pi h_0R}{4}e^{-i\theta_0}z_1\delta_{n,1}-\frac{(-i)^n n z_n}{2^n(n!)^2}\times\sum_{j\neq 0}\sum_{m=1}^{\infty}\left(\frac{R}{d_j}\right)^{n+m}e^{-i(n+m)\psi_j}\times(n+m-1)!(-2i)^m\beta_{-m}(j), \tag{33a}$$

whereas for $n<0$ we find

$$\beta_{-|n|}(0)=-\frac{\pi h_0R}{4}e^{-i\theta_0}z_{-1}\delta_{|n|,1}-\frac{(-i)^{|n|}|n|z_{|n|}}{2^{|n|}(|n|!)^2}\times\sum_{j\neq 0}\sum_{m=1}^{\infty}\left(\frac{R}{d_j}\right)^{|n|+m}e^{i(|n|+m)\psi_j}\times(|n|+m-1)!(-2i)^m\beta_m(j). \tag{33b}$$

The expressions in Eqs. (33) allow the analysis of the response of the array of nanowires to a spatially uniform magnetic field of frequency Ω, applied in the xy plane.

III. NUMERICAL STUDIES OF SPIN EXCITATIONS IN INTERACTING CYLINDER ARRAYS

In this section we present studies of the spin excitations in interacting arrays of cylinders. Two examples are considered. First, we consider two cylinders whose centers are separated by the distance d. This allows us to make contact with the exact treatment of the long wavelength magnetostatic modes presented in the Appendix, and to study some features of the interwire interactions for a simple system. Then, as a second example, we consider a linear array of ferromagnetic cylinders.

A. Interactions between two ferromagnetic cylinders

In what follows, we examine the spin excitations in two ferromagnetic cylinders, each with radius R and with their axes of symmetry separated by the distance d. All the numerical calculations employ a basis set where the azimuthal quantum number m extends from -30 to $+30$.

When the wave vector k is zero, the scaled equations may be used to calculate the spin wave normal modes of the cylinder pair, in the magnetostatic limit. Of course, this is precisely the limit in which the exact formula derived in the Appendix applies as well. We have tested Eqs. (17) by calculating the long wavelength spin wave frequencies of the cylinder pair, to find they indeed reproduce the result of the analytic formula very well.

The eigenvectors associated with the $k=0$ magnetostatic modes of the cylinder pair are very interesting. First, note from the discussion in the Appendix that for any given separation, we have two degenerate modes associated with the positive frequency solution given in Eq. (A8). One is associated with a positive value of the quantum number $m>0$, and one is associated with its negative $-m$. (Here we refer to the azimuthal quantum numbers in the bipolar coordinate system used in the Appendix, not to the azimuthal quantum number of the basis functions in polar coordinates used in Sec. II.) In the Appendix, it is noted that since reflections in the yz plane are not a good symmetry operation for the ferromagnetic cylinder pair by virtue of the axial vector character of the magnetization, the eigenvectors do not have well defined parity under this reflection. However, it is the case that the *product* of two reflections we may write as $R_{xz}R_{yz}$ is a good symmetry operation. R_{yz} interchanges the two cylinders and reverses the sign of the magnetization, while R_{xz} reverses the magnetization again to restore it to its original state. Thus, the product operation exchanges the two cylinders, and leaves the magnetization in its original state. The product $R_{yz}R_{xz}$ applied to the eigenvector of the positive frequency mode with quantum number $+|m|$ will generate the eigenvector associated with the mode $-|m|$. We illustrate this in Fig. 2, where we reproduce the lines of constant magnetic potential outside the cylinder pair as well as the in plane magnetization inside the cylinders, when the modes with $|m|=\pm 1$ are excited, for the case $d/R=2.5$. The asymmetry in each eigenvector is striking, with most of the excitation energy concentrated on one of the two cylinders in each case. Also, it is clear that as the two cylinders are brought together, the excitation localizes in the near vicinity of the points of closest contact between the two cylinders. As d/R approaches 2, the value where contact is established, the excitation becomes very localized indeed. In contrast, as d/R becomes very large, the $m=\pm 1$ (of bipolar coordinates) modes evolve into to $m=1$ modes (local polar coordinates) of single cylinders, centered at the left and right cylinders, respectively.

In Fig. 3(a), for the case $d=2.3R$, we show the dispersion relation of the two lowest lying magnetostatic spin wave branches of the cylinder pair, as a function of wave vector parallel to their axes. These have been calculated through use of Eq. (12) applied to this circumstance. We explored values of kR as small as 10^{-3}, again with a basis set where the azimuthal quantum number ranged from -30 to $+30$. It is remarkable in our view that accurate results can be obtained in the numerical work, when as noted above it is realized that for small values of its argument, $K_m(x)$ diverges as x^{-m}. In the determinant whose zeros one seeks to find the spin wave frequencies, the order of the modified Bessel function in-

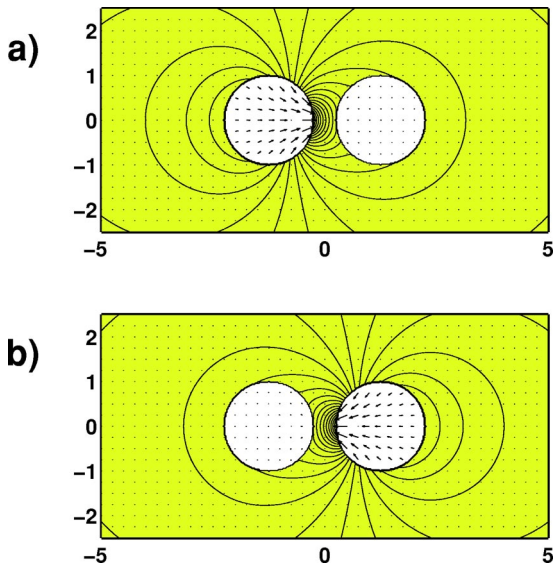

FIG. 2. For the case $d/R=2.5$, we show the eigenvectors of the $k=0$ magnetostatic mode of the cylinder pair for the case (a) $m=1$ and (b) $m=-1$: the lines of constant potential outside the cylinders and the in plane magnetization inside them. The two quantum numbers refer to the eigenvector expressed in the bipolar coordinates used in the Appendix. We have chosen $h=H_0/4\pi M_s=0.19$.

creases as one moves in the direction perpendicular to the diagonal. These objects become very large indeed in the outer portion of the entries, but in the end they influence the results very little when the basis set is sufficiently large to insure convergence. Again we find excellent agreement between the long wavelength limiting frequencies obtained from the full multiple scattering description of the cylinder pair, and the exact formula in the Appendix.

We see that each branch becomes twofold degenerate as $k\rightarrow 0$, whereas for finite wave vector the modes split. From the lower branch, it is evident that the splitting is largest when $kd\sim 1$, to decrease and eventually vanish in the limit $kd\gg 1$. The interactions between the cylinders is controlled by modified Bessel functions whose argument is kd and these vanish exponentially for large values of this variable, so at large wave vectors the cylinders are essentially decoupled. Notice the splitting of the second branch is very small, much smaller than that realized in the lowest branch. The angular variation of the magnetization in each cylinder has largely $m=2$ character for the second branch, while that in the lowest branch has largely $m=1$ character. Thus, at long wavelengths, when the lower branch is excited the inter-cylinder interaction has the character of a two-dimensional dipolar interaction, whereas the second branch is the next higher moment in the spirit of a multipole expansion. One interesting feature of Fig. 3(a) in our view is that the interaction between the cylinders, as judged from the splitting in the dispersion relation, is very modest in magnitude. The separation between the two is only 15% of their radius, for the calculations in Fig. 3(a). In Fig. 3(b), we show dispersion curves of the lowest two branches when the cylinders nearly

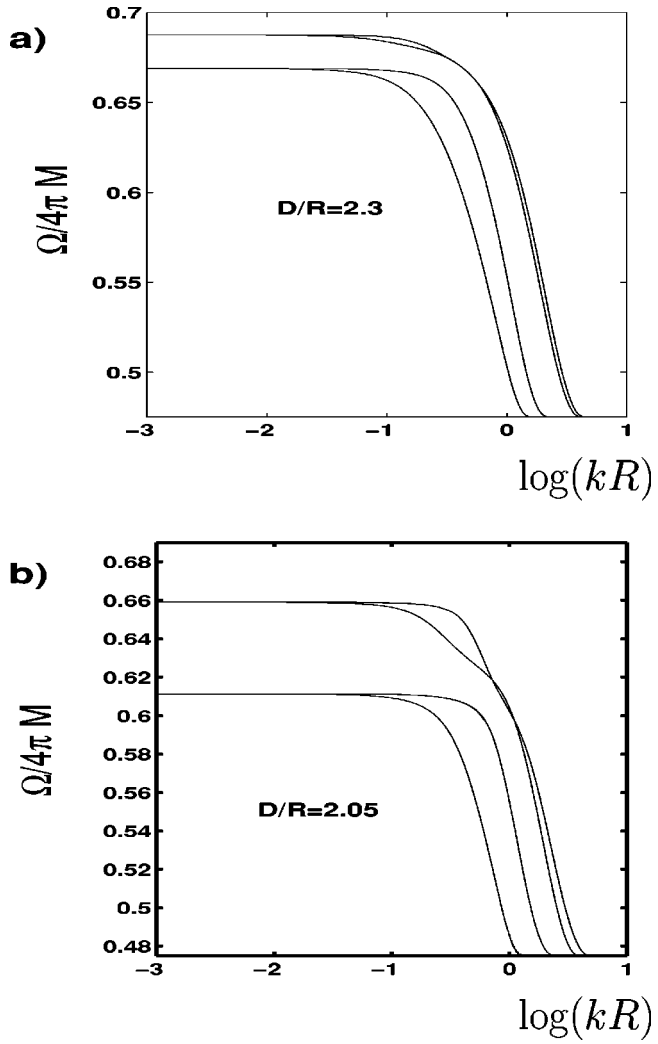

FIG. 3. For two cases, (a) $d/R=2.3$ and (b) $d/R=2.05$, we show the dispersion relation of the two lowest magnetostatic spin wave branches of the two nanowire cylinders. The calculations assume $H_0/4\pi M_s=0.19$, and the frequencies are given in units of $4\pi M_s$.

touch, with $d=2.05R$. Note the interesting structure and crossings in the dispersion curves of the second branch.

The influence of exchange can be characterized by the dimensionless parameter $p=(D/4\pi M_s R^2)^{1/2}$, with D the exchange stiffness. The system is exchange dominated when $p\gg 1$. In Fig. 4(a), with the influence of surface anisotropy ignored and when the cylinders are almost touching ($d=2.05R$), we show the two lowest lying spin wave branches of the cylinder pair for $p=0.5$. Again we see that as the wave vector vanishes, we have a two fold degeneracy, and splitting at finite wave vector. It is evident that exchange strongly suppresses interactions between the cylinders; in the lowest branch the splitting is very much smaller that evident in Fig. 3(b), and on the scale of the graph, the splitting is difficult to discern in the second branch, though it is indeed present for nonzero wave vectors. As before, the splitting is maximum in the region where $kd\sim 1$. In Fig. 4(b), we show the dispersion curve for the lowest branch when $p=2$, again with surface anisotropy ignored. Only the lowest branch is

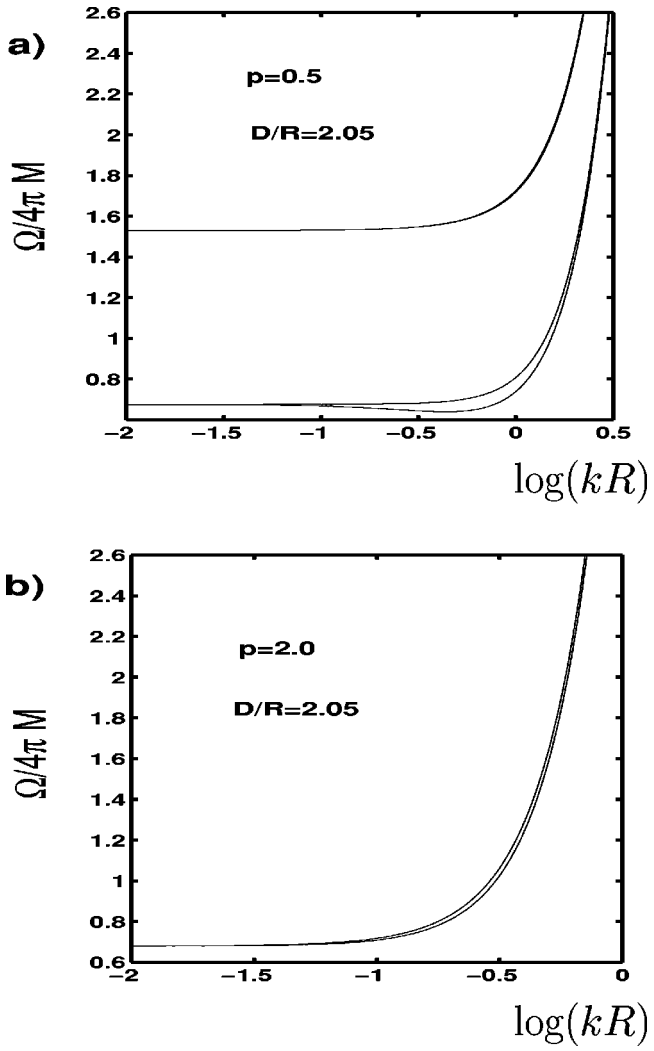

FIG. 4. We show the influence of exchange on the dispersion relations, for (a) $p=0.5$ and (b) $p=2.0$, $p=(D/4\pi M_s R^2)^{1/2}$ with D the exchange stiffness. Both calculations are for the choice $d/R=2.05$ where the cylinders almost touch. Again we have chosen $h=H_0/4\pi M_s=0.19$.

illustrated because now the exchange is strong enough that the second branch lies outside the frequency range covered in the plot. We see that increasing the strength of the exchange decreases the strength of the intercylinder interactions. In Fig. 5, for $p=0.5$ and wave vector such that $\log(kR)=-0.2$, we plot the splitting realized in the lowest spin wave branch as a function of separation between the centers of the two cylinders. We see a rather slow decrease of the splitting with d; the interaction between the pair has its origin in long ranged magnetostatic interactions and thus it falls off slowly with separation.

The calculations presented in Fig. 3 show that as the radius of the ferromagnetic nanowire decreases, to the point where the spin wave spectrum is importantly influenced by exchange, the interactions between nanowires is suppressed. The physical origin of this behavior can be appreciated from the eigenvector plots in Fig. 2. We see that as the cylinders are brought close together, the excitation concentrates around the points of closest contact between the cylinder pair. As we

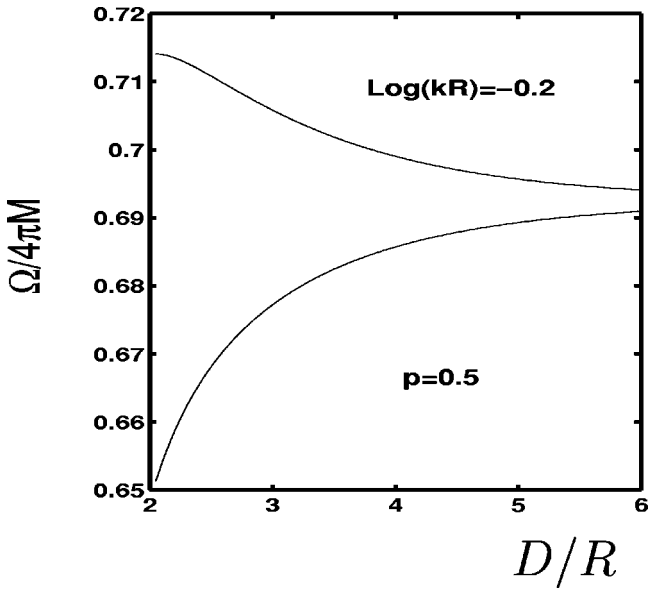

FIG. 5. For $p=0.5$ and $\log(kR)=-0.2$ we show the splitting in the lowest spin wave branch as a function of distance between the centers of the two cylinders. We have $h=H_0/4\pi M_s=0.19$.

''turn on'' exchange, this tendency will be opposed, with the consequence that the magnetic poles responsible for the magnetic fields which produce the coupling are spread out over a wider angular range. This decreases the strength of the magnetostatic interaction between nearby nanowires. We remark that all calculations reported here assume that the surface anisotropy vanishes. We have carried out calculations which incorporate rather strong surface anisotropy, to find that the interwire interactions remain modest in the limit of strong exchange. This conclusion is expected from the reasoning just given, of course.

B. Linear array of ferromagnetic cylinders

We now turn our attention to a periodic, linear array of ferromagnetic cylinders. The distance between the centers of two nearest neighbors is $d>2R$. We shall confine our attention to propagation perpendicular to the magnetizations of the cylinders. For the case of a uniform ferromagnetic film, this propagation geometry is of particular interest, because it is here that the much studied Damon Eshbach mode is realized. We note also that the BLS studies of collective excitations in a linear array of magnetic stripes[2] was carried out in this geometry as well.

For a period array of cylinders such as that just described, the coefficients $B_n(j)$ have the Bloch form $B_n(j)=B_n(0)\exp(ik_\perp dj)$, where $-(\pi/d)<k_\perp<\pi/d$. In the calculations below, when intrawire exchange is considered, we employ Eq. (12) with kR chosen very small, 10^{-3}. The scaled equations displayed as Eqs. (17) have proved most convenient for the discussion of the magnetostatic limit.

We begin with the limit where the intrawire exchange is appreciable, with the dimensionless parameter $p=0.5$. In Fig. 6(a), for the case where the cylinders are very close together with $d/R=2.05$, we show dispersion curves for the

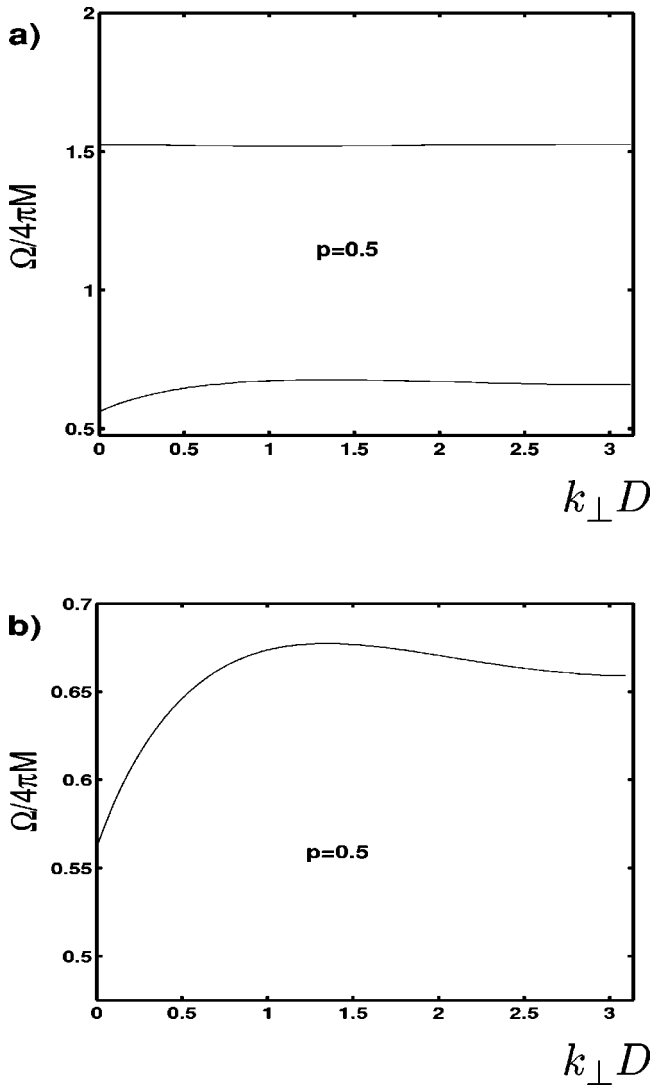

FIG. 6. For the periodic linear array of cylinders, and for the case where $d/R=2.05$ and with the exchange parameter $p=0.5$, we show (a) the dispersion relation of the two lowest collective modes, and (b) an expanded view of the dispersion relation of the lowest mode. We have $h=H_0/4\pi M_s=0.19$.

two lowest lying spin wave branches. As before, we have taken $h_0=H_0/4\pi M_s=0.19$, and the frequencies are expressed in terms of the dimensionless ratio $\Omega/4\pi M_s$. The upper branch in the figure is almost dispersionless, while we can see appreciable dispersion in the lowest branch. In Fig. 6(b), we show an expanded view of the dispersion curve associated with the lowest lying branch. Clearly we have a collective mode of the array of cylinders which in a qualitative, but surely not quantitative sense, reminds us of the Damon Eshbach mode of the uniform ferromagnetic film.[10] In the latter case, the mode exhibits a linear variation with wave vector at small wave vectors very much as we see in the dispersion curve in Fig. 6(b), but for the cylinders we see a maximum in the dispersion curve in the region $k_\perp d\sim 1$. For the uniform film, the dispersion relation is a monotonically increasing function of the wave vector.

As the strength of the exchange is weakened, the higher lying exchange branches decrease in frequency, until they

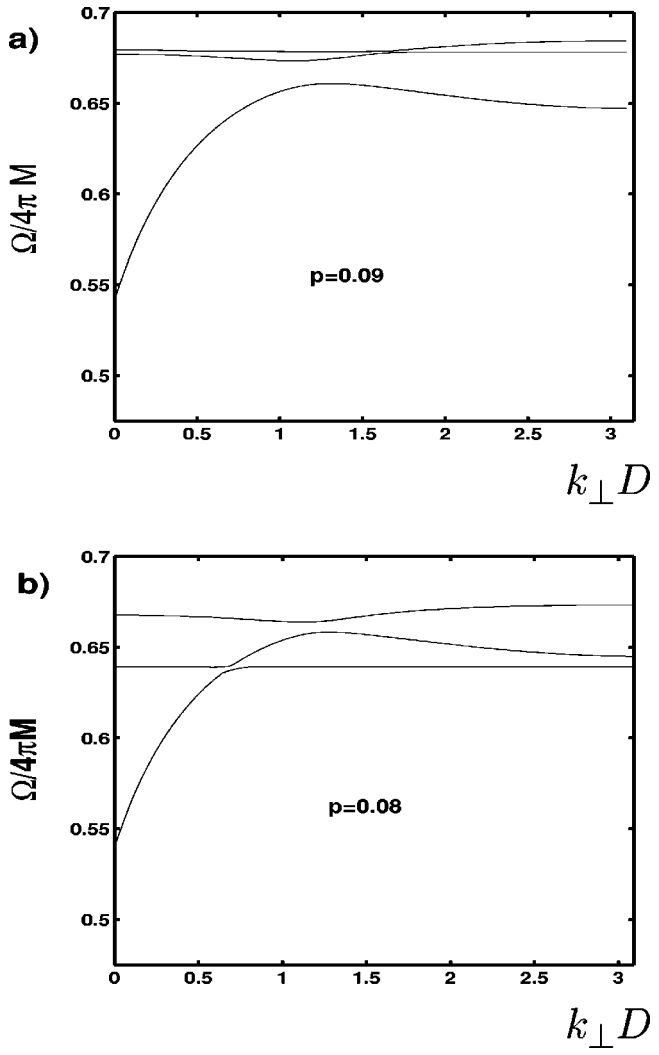

FIG. 7. Again for $d/R=2.05$ we show the two lowest lying branches for (a) $p=0.09$ and (b) $p=0.08$. We have $h=H_0/4\pi M_s=0.19$.

enter the frequency domain of the lowest lying collective mode branch. When they reach this regime, we see hybridization between the higher lying, rather flat branches and the highly dispersive lowest lying branch. We see this in Fig. 7(a) and 7(b). For $p=0.09$ [Fig. 7(a)], the second branch has quite not entered the frequency domain of the low lying collective mode, but by decreasing the strength of the exchange only slightly to $p=0.08$ we see clear hybridization between the two modes. By the time the exchange is lowered to $p=0.05$ we see several exchange branches mixing with the low lying collective mode, whose dispersion curve is clearly perceived as it passes through the hierarchy of exchange modes. We illustrate this in Fig. 8. In our view, the results in this figure bear a striking qualitative resemblance to the mode structures studied by BLS,[2] for a linear periodic array of magnetic stripes. The data showed a collective mode rather similar in nature to the Damon Eshbach mode of the uniform film, which crossed and hybridized with the standing wave exchange/dipole modes of the individual constituents.

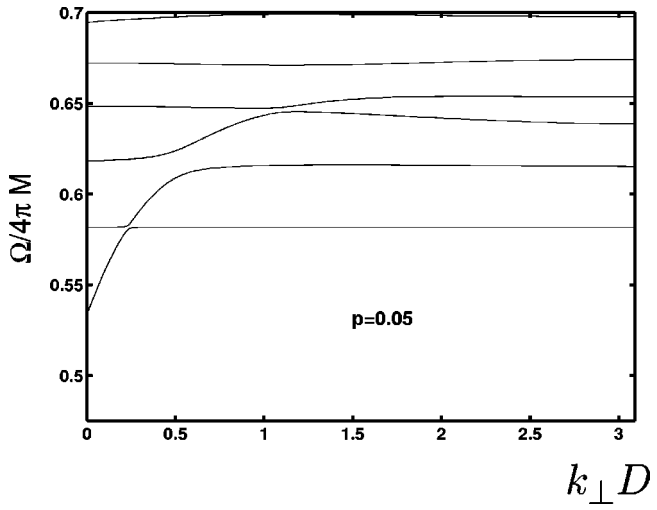

FIG. 8. For $d/R=2.05$ and $p=0.05$, we show the low lying collective modes of a linear array of ferromagnetic cylinders. We have $h=H_0/4\pi M_s=0.19$.

In the limit where the radius of the individual wires is sufficiently large that exchange may be ignored, and also in the limit where the wave vector parallel to the axis of symmetry of the cylinder vanishes, the surface magnetostatic modes of the isolated cylinder approach the limiting frequency $H_0+2\pi M_s$. These modes are characterized by an azimuthal quantum number m, and in the limit of zero wave vector parallel to the axis, we have an infinite number of degenerate modes at this frequency. In the long wavelength limit, the dispersion relation of these modes in Eqs. (6) of Ref. 4. The $m=1$ mode is the mode excited in FMR studies of ferromagnetic cylinders. As the cylinders are brought together, these modes interact, and we find a spectrum of collective modes outside and above the frequency $[H_0(H_0+4\pi M_s]^{1/2}$, below which one encounters standing spin waves. For $d/R=2.05$ and for $H_0/4\pi M_s=0.19$, in Fig. 9(a) we show the dispersion relation of the first few branches of these collective modes, for propagation perpendicular to the magnetization. As the cylinders are separated, the long wavelength limiting frequencies move up toward the limit $H_0+2\pi M_s$, and the bandwidths of the various modes are reduced. We illustrate this in Fig. 9(b), where we show the dispersion relations of the low lying collective modes for $d/R=2.2$, with all other parameters the same as used for Fig. 9(a).

We see that the linear array of ferromagnetic cylinders exhibits an array of collective modes; for the case where the wire diameter is sufficiently small that intrawire exchange drives the lowest standing exchange wave well above the magnetostatic mode spectral region, we have a highly dispersive low lying branch with behavior similar to, but nonetheless different in detail from the well know Damon Eshbach wave of the uniform film. As exchange is decreased in strength, we find hybridization between this collective mode, and the standing wave exchange modes of the individual constituents of the array, very similar in a qualitative sense to the behavior found in Brillouin light scattering studies of magnetic stripes.

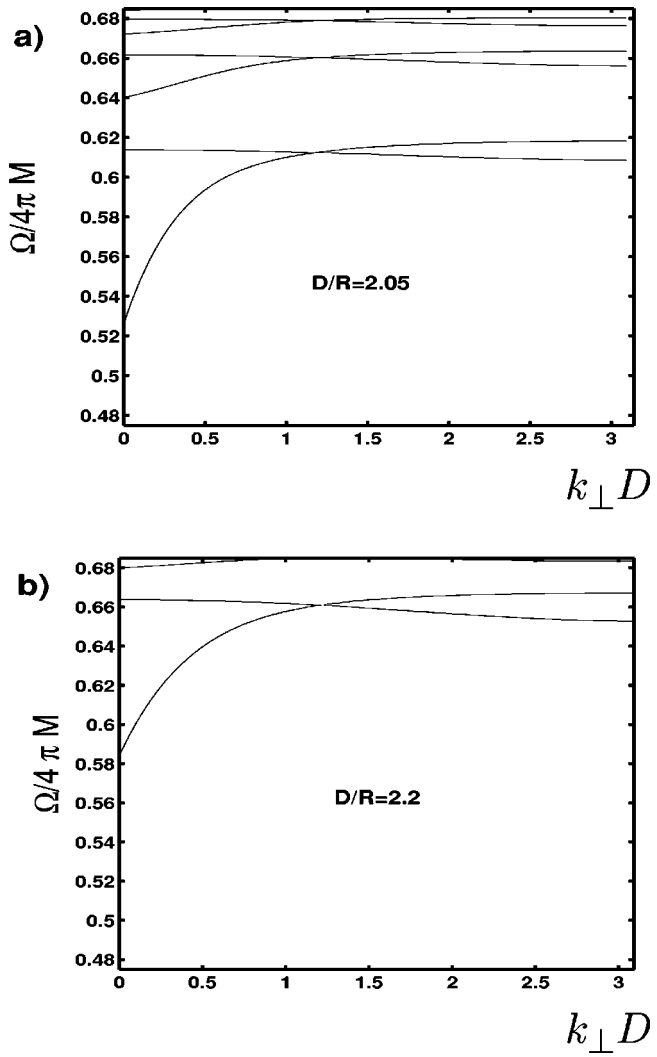

FIG. 9. In the magnetostatic limit, and for $h=H_0/4\pi M_s=0.19$, we show the dispersion curves for the collective modes of the linear cylinder array for (a) $d/R=2.05$ and (b) $d/R=2.2$. The propagation direction is perpendicular to the axes of the cylinders.

IV. CONCLUDING REMARKS

In this paper, we have presented a theoretical formulation of the response characteristics of arrays of interacting ferromagnetic nanowires, for the case where the wires have magnetization parallel to their symmetry axis, and their cross section is cylindrical. The formalism we have developed is a real space formalism based on multiple scattering theory, and as a consequence can be applied to disordered as well as ordered arrays of nanowires. We have developed both the theory of the collective excitations of such arrays, and their response to a microwave field. In the numerical calculations presented here, we have confined our attention to the nature of the collective excitations of selected systems, since at the time of this writing we do not have in hand experimental studies of the microwave response of suitable arrays.

We have explored two cases. One is the nature of the collective excitations of a pair of nanowires, of radius R separated by the distance $d>2R$. We have explored the nature of the collective exciations of such a pair of cylinders, as

a function of wave vector parallel to their symmetry axis. In addition, in the Appendix, we have obtained a closed form expression for the FMR frequency of such a pair, as a function of the distance between their centers. The message contained in our results is that the two nanowires have to be rather close together before their interactions become appreciable.

We have also examined the collective excitations of a periodic linear array of nanowires, for the case where the wave vector of the excitation is perpendicular to the axis of symmetry. We find results which are most striking in our view, which may be interpreted as a dispersive collective mode not unlike the well known Damon Eshbach mode of the uniform film, which crosses and hybridizes with the exchange/dipole resonances of the individual cylinders. The dispersions relations we obtain are quite similar in a qualitative sense to the modes of a linear array of magnetic stripes, studied through use of Brillouin light scattering spectroscopy.[2] Of course, in the experiments, the samples were very different in character than the model system studied here, in that the individual constituents were not cylinders, but rather magnetic stripes of rectangular cross section, with width very large compared to their height. Unfortunately, the formalism developed here cannot be extended to such structures in a straightforward way.

Our calculations of the collective excitations of the linear array of cylinders show that such structures posses a spectrum of collective modes that may be altered easily by changing the lattice constant of the array. It would be of interest to explore the spectrum of modes in a two dimensionally periodic array as well. In recent years, magnetic multilayers have been studied intensively, and these exhibit most interesting response characteristics that can be designed or altered by changes in microstructure. Ferromagnetic nanowire arrays may offer another very interesting class of systems that also may be synthesized in diverse forms, and the formalism developed here will allow the study of both their collective spin wave excitations and their response to a microwave field. It should be remarked that, through suitable adaptation, our description of the microwave response also forms the basis for a theory of the Brillouin light scattering spectrum.

ACKNOWLEDGMENTS

The research of D.L.M. was supported in part by the U. S. Army, through Contract No. CS0001028 and also by the Department of Energy through Grant No. DE-FG03-84ER-45083. The research of R.A. was supported by the Department of Energy grant just cited.

APPENDIX: ANALYTIC FORMULA FOR THE LONG WAVELENGTH MAGNETOSTATIC MODES OF TWO FERROMAGNETIC WIRES

Consider two ferromagnetic wires of cylindrical cross section, each of radius R separated by the distance d. Each has its axis of symmetry parallel to the z direction, one has its symmetry axis located on the x axis at $x=+d/2$, and the other has its symmetry axis located on the x axis as well, at $x=-d/2$. The geometry is thus different than that illustrated in Fig. 1.

We shall carry out the discussion in bipolar coordinates in the xy plane.[11] These are described in terms of two dimensionless coordinates (ξ,θ) and a length a, related to x and y by the statements

$$x=\frac{a\sinh(\xi)}{\cosh(\xi)+\cos(\theta)} \tag{A1a}$$

and

$$y=\frac{a\sin(\xi)}{\cosh(\xi)+\cos(\theta)}. \tag{A1b}$$

A contour of constant ξ is described by the statement, for $\xi>0$

$$(x-a\coth(\xi))^2+y^2=a^2/\sinh(\xi)^2, \tag{A2}$$

and is thus a cylinder with axis on the x axis located at $x=a\coth(\xi)$, with radius $a/\sinh(\xi)$. As the angular variable θ is swept from 0 to 2π, one executes a walk around the circumference of the cylinders just described. If $\xi>0$ the cylinder lies entirely in the half plane $x>0$, while it lies entirely in the half plane $x<0$ when $\xi<0$.

The two cylinders of interest are both contours of constant ξ. If we let $R=a/\sinh(\xi_0)$ and $d=2a\coth(\xi_0)$, then in bipolar coordinates the right hand cylinder is described by the statement $\xi=\xi_0$, while the left hand cylinder is described by $\xi=-\xi_0$. The interior of the right hand cylinder is the region $\xi>\xi_0$, the interior of the left hand cylinder is $\xi<-\xi_0$, while the remainder of the xy plane is covered by the range $-\xi_0<\xi<+\xi_0$.

Let us consider a spin wave excitation with wave vector k parallel to the z axis, and $\Phi_M(\xi,\theta)$ describe the variation of the magnetic scalar potential in the xy plane, when a normal mode of the coupled pair of cylinders is excited. Equation (1), when transformed to bipolar coordinates, reads

$$\left[\frac{\partial^2}{\partial\xi^2}+\frac{\partial^2}{\partial\theta^2}\right]\Phi_M(\xi,\theta)-h(\xi,\theta)^2k^2\Phi_M(\xi,\theta)=0, \tag{A3}$$

where $h(\xi,\theta)=a/[\cosh(\xi)+\cos(\theta)]$.

If we confine our attention to excitations of infinite wavelength with $k=0$, we have Laplace's equation in the variables (ξ,θ) and we have separable solutions of the general form $[A\exp(-a\xi)+B\exp(+a\xi)]\exp(ia\theta)$; since any solution of interest must be single valued in θ we must choose $a=m$, an integer. We seek a solution in the form (assuming that $m>0$)

$$\Phi_M(\xi,\theta)=A_m\exp(-m\xi)\exp(im\theta),\quad \xi>\xi_0, \tag{A4a}$$

$$\Phi_M(\xi,\theta)=B_m\exp(m\xi)\exp(im\theta),\quad \xi<\xi_0 \tag{A4b}$$

and

$$\Phi_M(\xi,\theta)=[C_m\cosh(m\xi)+D_m\sinh(m\xi)]\exp(im\theta),\quad -\xi_0<\xi<+\xi_0. \tag{A4c}$$

The choices in Eqs. (A4a) and (A4b) are dictated by the requirement that the potential be nonsingular at the centers of the two cylinders (at $\xi=+\infty$ and $\xi=-\infty$). As we move infinitely far from the origin, Eq. (4c) approaches, with (ρ,ϕ) polar coordinates in the plane,

$$\Phi_M \rightarrow (-1)^m \left[C_m + \frac{2ma}{\rho}\{-iC_m \sin(\phi) + D_m \cos(\phi)\} \right]. \tag{A5}$$

Far from the cylinder pair, the magnetic fields generated by the precession of the magnetizations thus have the character of dipole fields in two dimensions, since they fall off as ρ^{-2} as $\rho\rightarrow\infty$. The dipole is anisotropic, since in general $C_m \neq D_m$.

The boundary conditions on the cylinder surface are that tangential components of $\vec{H}$ are conserved, while normal components of $\vec{B}$ are conserved. We have

$$\vec{H} = -\vec{\nabla}\Phi_M = -\frac{\hat{\xi}}{h}\frac{\partial \Phi_M}{\partial \xi} - \frac{\hat{\theta}}{h}\frac{\partial \Phi_M}{\partial \theta}, \tag{A6}$$

while for conservation of normal $\vec{B}$ inside the cylinders we have $B_\xi = \mu_1 H_\xi + i\mu_2 H_\theta$, where if the cylinders are ferromagnets, μ_1 and μ_2 are defined in the main text just after Eq. (4). (As we shall note below, our treatment applies to antiferromagnetic and dielectric cylinders as well.)

The boundary conditions just stated lead us to four homogeneous equations for the coefficients in Eqs. (A4). Upon setting the appropriate determinant to zero, one obtains an implicit dispersion relation for the normal modes of the cylinder. This may be cast into the form

$$(\mu_1+1+\mu_2)(\mu_1+1-\mu_2) = -4\mu_1\left(\frac{1}{\exp(4|m|\xi_0)-1}\right), \tag{A7}$$

where $\cosh(\xi_0)=d/2R$.

For the case where the two cylinders are ferromagnets, and μ_1 and μ_2 are given by the expressions which follow Eq. (4) of the main text, it is possible to find explicit expressions for the frequencies of the modes. We find two frequencies for each value of m:

$$\Omega_m = \pm\left\{\frac{1}{4}[\Omega_B+\Omega_H]^2 - 4\pi^2\Omega_M^2 \exp(-4|m|\xi_0)\right\}^{1/2}. \tag{A8}$$

The result in Eq. (A8) is most striking in our view. First, as the cylinders are separated by a large distance, $(\xi_0\rightarrow 0)$, we recover the well known expression for the magnetostatic mode frequencies of the cylinder. When the wavelength $k\rightarrow 0$, these are all degenerate with the frequency $\Omega_m = \pm(1/2)(\Omega_B+\Omega_H) = \pm\gamma(H_0+2\pi M_s)$. It is the $m=1$ mode that is excited in ferromagnetic resonance,[4] so this last expression is also the FMR frequency of the isolated cylinder.

As the two cylinders are brought together, remarkably we do not see a splitting of the FMR mode, but rather just a frequency shift. The reason why this is so may be appreciated from our discussion of the $k\rightarrow 0$ limit in Sec. II A. Consider the $m=1$ mode (the FMR mode) of an isolated cylinder, for instance. We have one mode, $m=+1$ at the frequency $\Omega_{FMR}=\gamma[H_0+2\pi M_s]$, and we have the $m=-1$ mode at the frequency $-\Omega_{FMR}$. Now bring the two such cylinders together, supposing they are sufficiently far apart that $d\gg 2R$ to make the discussion simple. Equations (17) show that the $m=+1$ mode of the right hand cylinder couples only to the $m=-1$ mode of the left hand cylinder. Also the $m=+1$ mode of the left hand cylinder couples only to the $m=-1$ mode of the right hand cylinder. One obtains four new modes, but the two positive frequency modes necessarily have exactly the same frequency, and the two negative frequency modes also have exactly the same frequency as each other, and a frequency equal in magnitude to that of the positive frequency. Only two frequencies are displayed in Eq. (A8); if one considers the case $m<0$, one obtains two additional frequencies identical in value to those in Eq.(8).

Another remarkable feature of the result in Eq. (A8) is its behavior in the limit $d\rightarrow 2R$, where the cylinders just touch. Then $\xi_0\rightarrow 0$, and all frequencies approach the FMR frequency of a *film*, the well known formula $(\Omega_B\Omega_H)^{1/2}$.

It is the case as well that interactions between the two cylinders are remarkably weak, until they are very close together indeed. As an example, suppose $\Omega_B=3\Omega_H$, so the FMR frequency of the isolated cylinder is then $2\Omega_H$. If we have $d=2.1R$, so that the separation between the two cylinders is only 5% of their diameters, one has for the $m=1$ mode of the pair a frequency of $1.93\Omega_H$, i.e., a downshift from the frequency of the isolated cylinder of only 3%. This is surprising to us in view of the fact, as discussed in Sec. I and in Ref. 4, the FMR mode of the isolated cylinder generates a magnetic dipole field outside the cylinder.

We conclude with two comments. First, it is interesting that the expression for the magnetic potential in Eq. (A4c) has no well defined parity under reflection through the y axis. It consists of a linear combination of an even parity piece $[\cosh(m\xi)]$ and an odd parity piece $[\sinh(m\xi)]$. This has its origin in the gyrotropic nature of the response of the cylinder. Upon setting μ_2 to zero, one finds solutions of well defined parity, even or odd. One understands this as follows. In the case of the ferromagnet, μ_2 is nonzero by virtue of the presence of the spontaneous magnetization $\vec{M}=\hat{z}M_s$. If we reflect such cylinders in the yz plane, we must realize that the magnetization is an axial vector and changes sign upon reflection. Thus, reflection in the yz plane is not a good symmetry operation of the system.

We may apply Eq. (A7) to the discussion of the normal modes of antiferromagnets, as well as ferromagnets, by making the appropriate choice of μ_1 and μ_2. The antiferromagnet in zero external field has $\mu_2=0$, so here we have modes of well defined parity. Also, the result in Eq. (A7) may be applied to the discussion of the normal modes of cylinders which contain conduction electrons which exhibit a plasma response, possibly placed in an external magnetic field. To study this case, one replaces μ_1 and μ_2 by the appropriate frequency dependent elements of the dielectric tensor ε_1 and

ε_2. An interesting case is the simple plasma response, where $\varepsilon_2=0$ and $\varepsilon_1=\varepsilon_\infty-(\Omega_p/\Omega)^2$.[12]

Quite in contrast to the case of two ferromagnetic cylinders brought together, the plasmon modes of the cylinder pair display a splitting, with frequencies

$$\Omega_m(\pm)^2=\frac{\Omega_p^2}{(\varepsilon_\infty+1)^2+\varepsilon_\infty f(|m|\xi_0)}\left[\varepsilon_\infty+1+\frac{1}{2}f(|m|\xi_0)\pm\left\{f(|m|\xi_0)+\frac{1}{2}f(|m|\xi_0)^2\right\}^{1/2}\right], \tag{A9}$$

where $f(x)=1/[\exp(4x)-1]$. When the two cylinders are very far apart ($f(m\xi_0)\to 0$), we have two degenerate modes at the plasma resonance frequency of the isolated cylinder, $\Omega_p/(\varepsilon_\infty+1)^{1/2}$, and when they are brought together so they just touch [$f(m\xi_0)\to\infty$], one mode is driven up in frequency to $\Omega_p/\varepsilon_\infty^{1/2}$, which is the bulk plasma frequency of the material from which the cylinders are fabricated. The second mode is driven down to zero frequency, and becomes a long wavelength acoustic mode of the cylinder pair. These two modes each have a well defined parity.

[1] M. Natali, I. L. Prebeanu. A. Lebob, L. D. Buda, K. Ounadjela, and Y. Chen, Phys. Rev. Lett. **88**, 157203 (2002).

[2] See the discussion in S. O. Demokritov, B. Hillebrands, and A. N. Slavin, Phys. Rep. **348**, 442 (2001).

[3] U. Ebels, J. L. Duvail, P. E. Wigen, L. Piraux, L. D. Buda, and K. Ounadjela, Phys. Rev. B **64**, 014421 (2001).

[4] R. Arias and D. L. Mills, Phys. Rev. B **63**, 134439 (2001); **66**, 149903(E) (2002).

[5] Z. K. Wang, M. H. Kuok, S. C. Ng, D. J. Lockwood, M. G. Cottam, K. Nielsch, R. B. Wehrspohn, and U. Gosele. Phys. Rev. Lett. **89**, 027201 (2002).

[6] See Sec. II of Rodrigo Arias and D. L. Mills, Phys. Rev. B **60**, 7395 (1999).

[7] D. Felbacq, G. Tayeb, and D. Maystre, J. Opt. Soc. Am. A **11**, 2526 (1994).

[8] J. L. Lin, D. Y. Petrovykh, A. Lirakosian, H. Rauscher, F. J. Himpsel, and P. A. Dowben, Appl. Phys. Lett. **78**, 829 (2001).

[9] See identity 2 in Sec. 8.53, p. 979 of *Table of Integrals, Series and Products*, edited by I. S. Gradsheteyn and I.M. Rhyzhik (Academic Press, New York, 1965).

[10] See the discussion in Sec. 3 of D. L. Mills, in of *Surface Excitations*, edited by R. Loudon (Elsevier, Amsterdam, 1984), Chap. 2. The case of a film is discussed at the end of Sec. 3.

[11] *Mathematical Methods in Theoretical Physics*, edited by P. M. Morse and H. Feshbach (McGraw Hill, New York, 1953), p. 1210.

[12] See Appendix 1 of D. L. Mills and E. Burstein, Rep. Prog. Phys. **37**, 817 (1974).